ORIGINAL ARTICLE
Iran J Allergy Asthma Immunol
April 2026; 25(2):234-250.
DOI: 10.18502/ijaai.v25i2.20802

Dual Blockade of PD-L1 and AXL: A Novel Immunotherapeutic Approach for Ovarian and Cervical Cancer

Hossein Rahavi[1,2], Ahmad Najafi[3], Hossein Asgarian-Omran[1], Behrouz Aflatoonian[2], Mohsen Tehrani[1], and Ehsan Farashahi-Yazd[2]

[1] Department of Immunology, School of Medicine, Mazandaran University of Medical Sciences, Sari, Iran
[2] Stem Cell Biology Research Center, Yazd Reproductive Sciences Institute, Shahid Sadoughi University of Medical Sciences, Yazd, Iran
[3] SABA Biomedicals Knowledge-Enterprise Co, Tehran, Iran

Received: 19 May 2025; Received in revised form: 18 July 2025; Accepted: 1 August 2025

ABSTRACT

Tumor microenvironment modulators have produced durable effects in cancer treatment. Targeting immune checkpoint receptors, such as *PD-L1*, has demonstrated efficacy in eliciting antitumor responses. However, resistance to immune checkpoint blockers (ICBs) has constrained the efficacy of these therapies. Previous studies showed a link between the expression of *AXL* receptor tyrosine kinase and resistance to ICBs. Therefore, designing combination treatments with synergistic mechanisms to overcome ICB-based resistance is needed. In addition to antibody-based therapies, gene silencing with siRNAs has recently been explored to alter the cancer environment to enhance the immune response.

In this study, we targeted *PD-L1* using an siRNA and *AXL* using a blocker (R428) in OVACAR-3 and CaSki cells, ovarian and cervical cancer cell lines, respectively, in the following groups: Scramble-siRNA, PD-L1-siRNA, Scramble-siRNA in conjunction with R428, PD-L1-siRNA in conjunction with R428, R428 monotherapy and untreated controls. Cell viability was assessed by MTT assay after 48 hours of treatment, and cisplatin sensitization was evaluated in resistant OVACAR-3 cells. Gene expression was analyzed by qRT-PCR, while flow cytometry quantified $CD44^{+}PD\text{-}L1^{+}$ populations, apoptosis (Annexin V/PI), and cell cycle distribution.

The results showed a significant decrease in cell proliferation, suppression of EMT-regulating genes, reduction of stemness in cancer cells, increased apoptosis and disruption of the cell cycle in the studied cell lines.

These findings suggest that simultaneous blockade of *PD-L1* and *AXL* could serve as a novel tumor-suppressive strategy, especially for cancer patients resistant to ICBs.

Keywords: Axl receptor tyrosine kinase; Cervical cancer; Molecular targeted therapies; Ovarian cancer; Programmed death ligand 1; siRNA

Corresponding Authors: Ehsan Farashahi-Yazd, PhD; Stem Cell Biology Research Center, Yazd Reproductive Sciences Institute, Shahid Sadoughi University of Medical Sciences, Yazd, P.o.B: 89168-77391, Iran. Tel: (+98 35) 3824 7085, Fax: (+98 35) 3824 7085, Email: ehsanfarashahi@gmail.com

Mohsen Tehrani, PhD; Department of Immunology, School of Medicine, Mazandaran University of Medical Sciences, Sari, P.o.B: 48471-91971, Iran. Tel: (+98 11) 3354 3248, Fax: (+98 11) 3354 3081, Email: drmtehrani@gmail.com

INTRODUCTION

Gynecologic cancers are among the most common types of cancer worldwide. Among them, cervical cancer and, especially, ovarian cancer are leading causes of cancer-related deaths in women due to chemotherapy resistance. Despite advances in surgery and chemotherapy, many patients still succumb to aggressive disease variants. The high mortality rate and the impact on women's quality of life and fertility highlight the urgent need for novel treatments, such as immunotherapy.[1,2] Numerous studies have shown that targeting tumor-promoting elements within the tumor microenvironment can enhance anticancer immune responses and mitigate chemotherapy resistance.[3] Programmed cell death ligand 1 (*PD-L1*) is an immunosuppressive protein highly expressed on the surface of tumor cells, where it interacts with programmed cell death receptor 1 (*PD-1*) on T-cells. Following receptor-ligand interaction, T-cell proliferation and migration are suppressed, facilitating tumor growth and metastasis, while reducing the effectiveness of the antitumor response.[4]

Immune-checkpoint blockade (ICB) therapies targeting *PD-L1* have emerged as a promising new class of antitumor agents. However, they cannot counteract resistance mechanisms, and the number of patients who benefit from ICB-based immunotherapy remains limited.[5] AXL, a receptor tyrosine kinase (RTK) belonging to the TAM family (Tyro3, Axl, Mer), was initially identified as a transforming gene in cells from patients with chronic myelogenous leukemia.[6,7]

Subsequent studies revealed its crucial role in the progression of various tumors, as it contributes to epithelial-mesenchymal transition (EMT), facilitating metastasis and chemoresistance, while also influencing immune regulation within the tumor microenvironment (TME).[8]

Previous studies have linked *AXL* expression to resistance against ICB-based immunotherapy in both tumor models and cancer patients.[8–10] Researchers have recently focused on combination targeted therapies, since they induce the synergistic effects of targeted agents and increase the specificity of treatment.[11,12]

Over the past decades, the efficacy of ICBs combined with tyrosine kinase inhibitors has been discussed in both preclinical and clinical studies on different cancers.[13–15] Nonetheless, some patients have experienced unexpected complications during anti-PD-1/PD-L1 immunotherapy due to off-target antibody binding and autoimmune reactions.[5] Given the localization of *PD-L1* in several cellular compartments, which affects cancer treatment outcomes,[16] non-coding RNA molecules, such as small interfering RNA (siRNA), have attracted considerable research attention for developing targeted and effective therapies.[17,18] Furthermore, the delivery of siRNA not only reduces *PD-L1* expression but also prevents de novo *PD-L1* expression, hence diminishing tumor cell evasion and enhancing PD-1/PD-L1 blockade.[19] Both *PD-L1* and *AXL* are highly expressed in the TME of various cancers, including ovarian and cervical cancer, where their blockade has demonstrated impressive antitumor effects.[20,21] Therefore, the aim of this study was to explore the antitumor effects of treatment with PD-L1 siRNA and R428 (an AXL inhibitor) in ovarian and cervical cancer cells. This strategy is expected to exert synergistic antitumor effects in advanced-stage tumors, especially in ICB-resistant patients.

MATERIALS AND METHODS

Reagents and Antibodies

Bemcentinib (R428), a tyrosine kinase inhibitor, was obtained from MedChemExpress (New Jersey, Princeton, USA). This chemical compound was dissolved in 0.1% dimethyl sulfoxide (DMSO) and stored frozen in aliquots. Commercial types of siRNA (denoted as “si”), including Scramble-si, MALAT-1-si, and PD-L1-si, and the Lipofectamine RNAiMAX (LPs) as a transfection reagent, were ordered from Thermo Fisher Scientific (Massachusetts, USA). The viability assay was conducted using an MTT assay kit (Sigma-Aldrich, Merk Group, USA). PerCP/Cyanine5.5 anti-human CD274 (B7-H1, PD-L1) and PE anti-mouse/human CD44, as well as the Annexin V-FITC/PI Apoptosis Kit for cell death evaluation, were acquired from BioLegend (San Diego, CA).

Cell Lines and Culture

OVACAR-3 and SKOV3, as ovarian cancer cell lines, along with the CaSki and HeLa, as cervical cancer cell lines, were obtained from the Pasteur Institute (Tehran, Iran). Cells were cultured in DMEM and RPMI-1640 media, respectively, supplemented with 10% heat-inactivated fetal bovine serum (FBS) and 1%

penicillin/streptomycin (Gibco/Life Technologies, Grand Island, NY) under conditions of 37°C, humidified, and 5% CO_2. Upon achieving appropriate confluency, the cells were sub-cultured, and subsequent analyses were conducted during the logarithmic phase of growth.

R428 Treatment and PD-L1 Silencing

OVACAR-3 and CaSki cells were seeded into a 96-well plate at densities of 1×10^4 and 1.5×10^4 cells per well, respectively, and incubated at 37°C in a humidified atmosphere with 5% CO_2. To define the optimal concentration of R428, the cells were treated at ascending concentrations up to 20 µM of R428 for 24, 48, and 72 hours. Optimal concentration or half-maximal inhibitory concentration (IC_{50}) values were calculated for all drugs using GraphPad Prism version 8 (GraphPad Software, San Diego, CA, USA) curve-fitting software. To optimize the condition of *PD-L1* knockdown, cells were cultured at 5×10^4 and 7.5×10^4 in a 24-well plate and grown to 80% confluency. Then, OVACAR-3 and CaSki cells were transfected with 10 and 20 nM of PD-L1-si, respectively, for 24 and 48 hours. Quantitative reverse transcription polymerase chain reaction (qRT-PCR) was utilized to quantify the mRNA expression of *PD-L1* in siRNA-transfected cells. An siRNA targeting metastasis-associated lung adenocarcinoma transcript 1 (MALAT-1), a long non-coding RNA, was also used as a positive control to assess transfection efficiency. OVACAR-3 and CaSki cell lines in 24-well plates were transfected with scramble siRNA-loaded LPs (10 nM) and MALAT-1-si-loaded LPs (20 nM and 10 nM, respectively) for 48 hours. The *MALAT-1* mRNA expression level was identified using qRT-PCR.

In all experiments, treatments included scramble-si loaded LPs, PD-L1-si loaded LPs, scramble-si loaded LPs + R428, PD-L1-si loaded LPs + R428, R428, and non-treated cells. For the MTT assay, 0.2% DMSO as the positive control was also considered. Firstly, for transfection experiments, the cells were serum-starved for 3 hours. The optimum concentration of siRNA was diluted in 50 µL Opti-MEM I reduced serum medium (Opti-MEM, Invitrogen, USA) and mixed with 1 µL of Lipofectamine RNAiMAX pre-diluted in 50 µL Opti-MEM and incubated for 15 minutes at room temperature. The complexes were added to the cells in the desired volume of antibiotic-free RPMI-1640 medium. Combination treatment was conducted with 10 and 20 nM of PD-L1-si-loaded LPs and subsequently 2.6 and 2.1 µM of R428 for OVACAR-3 and Caski cell lines, respectively. The effects of the treatments on the studied cells were then evaluated using the MTT assay, qRT-PCR, and flow cytometry.

Cell Viability Assay

Cell viability was evaluated after co-treatment with PD-L1-si and R428 on OVACAR-3 and Caski cell lines by MTT assay (Sigma Aldrich, China). Briefly, OVACAR-3 and Caski cell lines were seeded in 96-well plates at a density of 1×10^4 and 1.5×10^4, respectively, and grown overnight to approximately 80% confluence. The cells were transfected using 10 µL of siRNA-loaded LPs (containing 10 nM siRNA) in each well with antibiotic-free RPMI-1640 medium. After 6 hours of incubation, the primary medium was substituted with fresh medium containing the optimized concentration of R428. After 48 hours of incubation (37°C, humidified, 5% CO_2), the supernatant from each well was removed and replaced with serum-free medium (100 µL) and MTT solution (10 µL) and incubated for an extra 4 hours in the dark. In the final step, 100 µL of DMSO was added to each well after aspiration of 110 µL of medium from each well, and plates were re-incubated for 30 minutes. The viability of cells was assessed by measurement of the plate absorbance with an ELISA reader at 570 nm versus 630 nm (reference value) wavelengths.

Cisplatin Sensitization in Resistant Cells

The combined effects of PD-L1-siRNA and R428 on the cisplatin resistance of OVACAR-3 cells were investigated. Firstly, IC_{50} values of cisplatin were determined for OVACAR-3 and human foreskin fibroblast (HFF) lines as a normal cell. For the main experiment, 1×10^4 OVACAR-3 cells were seeded into a 96-well plate and grown at 37 °C, humidified, and 5% CO_2. Then, various treatment strategies were applied on OVACAR-3 cells. Following 48 hours of incubation, the MTT assay was done as previously described, and cell viability was determined by measuring plate absorbance with an ELISA reader.

Gene Expression Analysis

In brief, OVACAR-3 and Caski cells (1×10^4 & 1.5×10^4) were subsequently treated in 24-well plates with the optimized concentration of siRNA and R428. After 48 hours, the total RNA extraction was performed by RiboEX reagent (GeneAll Biotechnology, Seoul, Korea) based on the manufacturer's instructions, and

then complementary DNA (cDNA) was synthesized using the Yekta Tajhiz cDNA synthesis kit (Tehran, Iran). qRT-PCR was carried out in a Rotor-Gene Q Real-Time PCR System (Qiagen, Maryland, USA) using SYBR green as the detection dye (Yekta Tajhiz, Tehran, Iran). The primer efficiencies were confirmed by standard curves following the reaction. Finally, the relative gene expression of *AXL*, *PD-L1*, transforming growth factor beta (*TGF-β*), *Vimentin*, and Matrix metalloproteinase-9 (*MMP-9*) was calculated compared to Hypoxanthine-guanine phosphoribosyl transferase (*HPRT)* as the reference gene. Melt curve and $2^{-\Delta\Delta CT}$ method were used to infer the results. The specific primer sequences are provided in supplemental table 1.

Immunophenotyping

To evaluate the effect of the combinational treatment on invasive properties of cancer cells, the frequency of $CD44^{+}PD\text{-}L1^{+}$ cells was determined by flow cytometry using CD44-allophycocyanin (APC), PD-L1-PerCP-Cy5.5, and isotype-matched control mAbs (BioLegend, USA) in comparison to non-treated cells. Briefly, 5×10^4 treated cells were suspended in 50 µL of staining buffer and incubated with optimized amounts of fluorochrome-conjugated mAbs at 4°C for 30 minutes. After washing twice with phosphate-buffered saline (PBS), stained cells were evaluated by FACS Calibur flow cytometer (BD, Biosciences, USA) and analyzed using FLOWJO software.

Apoptosis Assay

Apoptosis-mediated cell death was examined to explore the effect of the proposed treatment on the cells. The cells (5×10^4) were treated with PD-L1-si and R428 in a 24-well plate. After 48 hours of incubation, the cells were harvested and treated with a dual-color FITC-labeled Annexin V/propidium iodide (PI) apoptosis detection kit according to the protocol (BD Biosciences, USA). Finally, the externalization of phosphatidylserine and the permeability to PI were evaluated using a FACS Calibur flow cytometer (BD, Biosciences, USA).

Cell Cycle Analysis

Flow cytometry was used to evaluate the combinational treatment effect on the cell cycle. The cells were seeded into a 24-well plate at a density of 5×10^4 cells/well and treated with siRNAs and R428. After 48 hours, cells were detached, washed with cold PBS, stained with propidium iodide solution (PI, 50 µg/mL) and incubated in a dark place for 30 minutes. Finally, G0/G1, S, and G2 phases in the treated and control groups were assessed by FACS Calibur flow cytometer (BD, Biosciences). Cell cycle distribution was evaluated by FlowJo software.

Statistical Analysis

Statistical analyses were performed with GraphPad Prism 8 software. Quantitative data are expressed as mean ± SD. Analysis was performed using the Shapiro-Wilk test to determine the normality distribution of the obtained data, and one-way analysis of variance (ANOVA) followed by the Dunnett test for multiple comparisons. The results are expressed as the mean ± SD of three independent experiments. $p<0.05$ was considered statistically significant. $*p<0.01$ and $***p<0.001$ were considered extremely significant.

RESULTS

OVACAR-3 and CaSki Cells Showed High Levels of AXL and PD-L1 Expression

We analyzed the *AXL* and *PD-L1* expression levels in OVACAR-3 and SKOV3 cells along with CaSki and HeLa cell lines. As presented in Figure 1A and 1B, qRT-PCR results indicated that OVACAR-3 and Caski cells significantly exhibited the highest levels of *AXL* and *PD-L1* expression in comparison to the other cell lines. Furthermore, gene expression analysis confirmed the acceptable level of *TGF-β*, *vimentin*, and *MMP-9* genes in these cells (Figure 1E–G). Although, compared to OVACAR-3, the Caski cells showed the higher level of these genes (Figure 1C–G). Therefore, subsequent experiments were performed on these cell lines.

Downregulation of PD-L1 in OVACAR-3 and CaSki Cells Following siRNA Transfection

Transfection of PD-L1-si significantly reduced *PD-L1* gene expression in OVACAR-3 and CaSki cells at 10 and 20 nM, respectively. To identify the optimum time for transfection, PD-L1-si was transfected in a time-dependent manner (24 and 48 hours) in the cells. Compared to the scramble group, PD-L1-si was more effective in the knockdown of *PD-L1* expression at 48 hours of transfection time in both cells (Figure 2A). Therefore, the following tests were adjusted at 10 and 20 nM for OVACAR-3 and CaSki cells, respectively, as the optimum dose and 48 hours as the optimum time. Transfection efficiency of siRNA loaded on

lipofectamine was detected by qRT-PCR, where MALAT-1-si was utilized as a positive control for confirmation of siRNA-mediated knockdown. Figure 2B demonstrates that MALAT-1-si significantly suppressed expression of *MALAT-1* mRNA in both cell lines. Nearly 70% of the *MALAT-1* mRNA was inhibited at concentrations of 20 and 10 nM of siRNA in OVACAR-3 and CaSki cells, respectively, in a transfection time of 48 hours. These results showed that lipofectamine could deliver MALAT-1-si into cancer cells efficiently to further down-regulate the *MALAT-1* mRNA expression.

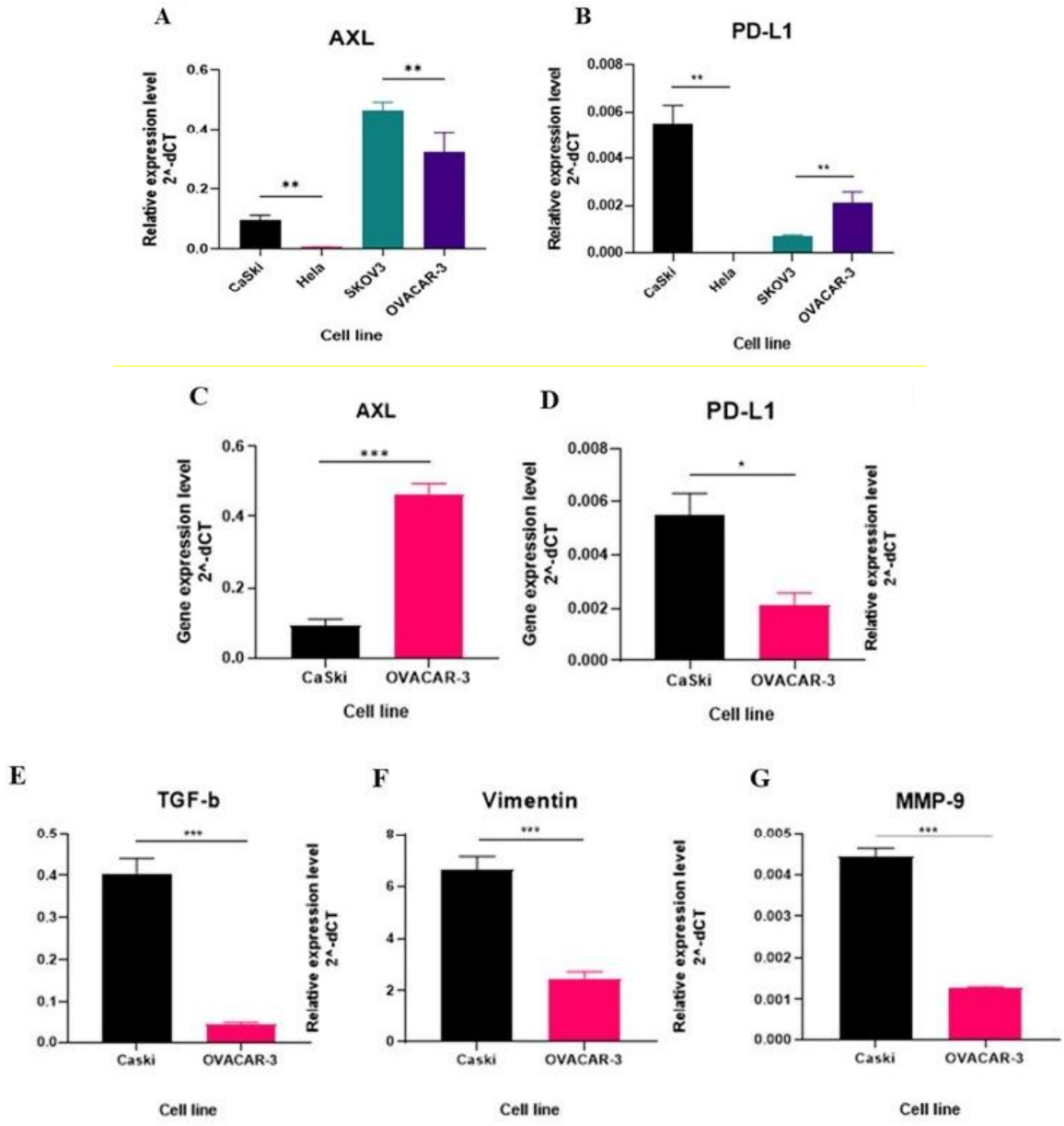

Figure 1. *AXL*, *PD-L1*, *TGF-β*, *vimentin* and *MMP-9* are highly expressed in OVACAR-3 and CaSki cells.
A. and B. OVACAR-3 and Caski cells exhibited significantly higher expression levels of *AXL* and programmed cell death-ligand 1 (*PD-L1*) compared to the other cell lines. C–G. qRT-PCR confirmed the expression of transforming growth factor beta (TGF-β), *vimentin*, and matrix metalloproteinase-9 (MMP-9) in the studied cell lines. Gene expression results are represented as mean ± SD of $2^{-\Delta\Delta Ct}$ after normalization with hypoxanthine-guanine phosphoribosyl transferase (HPRT) as an internal control. (p*<0.01, ***p*<0.005, ****p*<0.0001, NS:).**

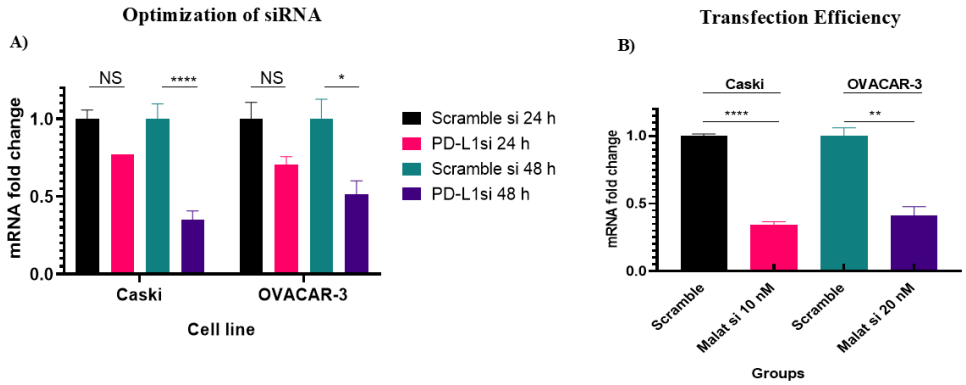

Figure 2. *PD-L1* knockdown in OVACAR-3 and CaSki cells. A. PD-L1-siRNA transfection reduced *PD-L1* gene expression in a time-dependent manner in both cell lines compared to the scramble group. B. MALAT-1-siRNA was transfected into the cells and effectively suppressed expression of metastasis-associated lung adenocarcinoma transcript 1 (MALAT-1) mRNA in both cell lines. Gene expression results are represented as mean ± SD of $2^{-\Delta\Delta Ct}$ after normalization with *HPRT* as an internal control (p*<0.05, ***p*<0.005, *****p*<0.0001).**

OVACAR-3 and CaSki Cell Lines Showed Reduced Proliferation Following Dual Blockade of PD-L1 and AXL

The effects of PD-L1-si and R428 on growth inhibition were examined in the OVACAR-3 and CaSki cell lines. Firstly, cell viability was measured via MTT assay following 24, 48, and 72 hours of exposure to various concentrations of R428. As shown in supplemental Figure 1, after a single exposure to R428 at concentrations up to 20 µM, OVACAR-3 and CaSki cells indicated a dose-dependent reduction in viability, with an IC_{50} value of 2.6 µM and 2.1 µM, respectively. In the next step, we measured the anti-proliferative activity of single or combined treatment by MTT assay using the calculation of the relative cell proliferation index for all samples. In this experiment, we found that the proliferation of both cell lines was significantly reduced in PD-L1-si and R428 as single treatment groups. As expected, co-treatment with PD-L1-si + R428 led to an enhanced cell growth inhibition when compared to a single treatment in both cell lines (Figure 3A).

Treatment with PD-L1-si and R428 Was Insufficient to Reduce Cisplatin Resistance in OVACAR-3 Cell Line

The OVACAR-3 cell lines were previously identified as a drug-resistant cancer cell.[22,23] Firstly, to assess the resistance levels of cisplatin, this drug alone was tested in OVACAR-3 and HFF as normal cells. IC_{50} (15.5 µM) was found to be sevenfold higher in resistant cells compared with the normal cells (supplemental Figure 2). To overcome cisplatin resistance in OVACAR-3 cells, six treatment strategies were appointed. The cell viability assay showed that a single treatment with cisplatin at a concentration below the IC_{50} did not inhibit cell proliferation compared with treatment at the IC_{50} concentration. Combination treatment with PD-L1-si and R428 at IC_{50} concentrations (10 nM and 2.6 µM, respectively) significantly reduced cell proliferation. However, when used at concentrations below their IC_{50} (5 nM and 1.3 µM, respectively) along with cisplatin (7.75 µM; at concentrations below its IC_{50}), the treatment neither reduced cell proliferation nor overcame cisplatin resistance in the OVACAR-3 cell line (Figure 3B).

Downregulation of EMT Regulating Genes Following Dual Blockade of PD-L1 and AXL

To further understand the molecular events underlying immune escape and the EMT-related mechanisms in the combination group, the expression of *PD-L1*, *TGF-β*, *vimentin*, and *MMP-9* was studied on OVACAR-3 and CaSki cell lines. Relative mRNA expression was evaluated using qRT-PCR, with *HPRT* as an internal control. The results demonstrated that the expression of *PD-L1*, *TGF-β*, and *MMP-9* was dramatically reduced on both cell lines after treatment with PDL-1si and R428 when compared to the scramble-si + R428 group even though OVACAR-3 cells exhibited a lesser reduction (Figure 4A, 4B, and 4D). In contrast, despite the significant decrease in *vimentin* in CaSki cells, the combined treatment failed to markedly diminish the expression of this gene in the OVACAR-3 cell line (Figure 4C).

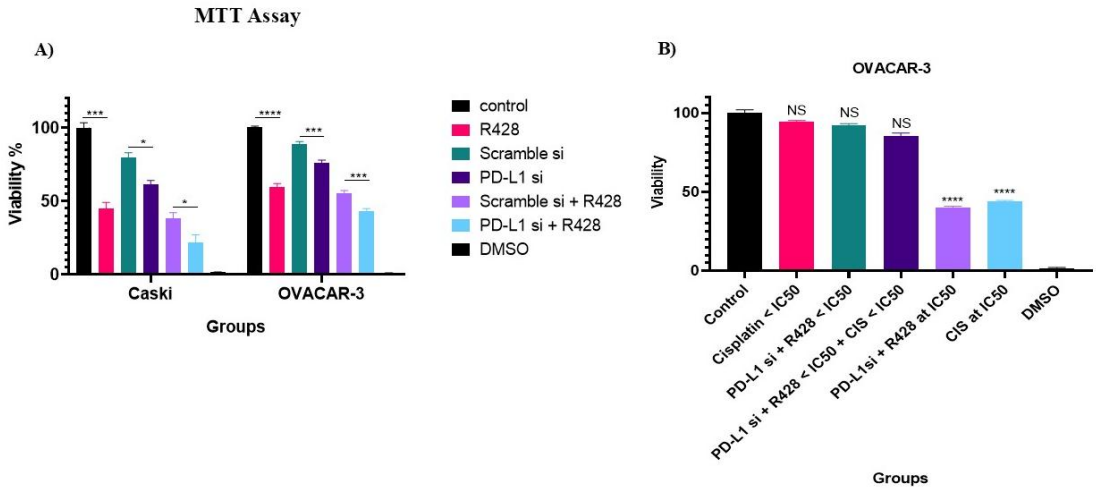

Figure 3. Proliferation of OVACAR-3 and CaSki cells following treatment with PD-L1-siRNA and R428. A. Treatment with PD-L1-siRNA and R428 led to significantly reduced proliferation when compared to a single treatment in both cell lines. B. OVACAR-3 cells, a drug-resistant cell line, were subjected to various treatments including PD-L1si (10 nM) and R428 (2.6 µM, as the IC_{50} concentration), PD-L1-si (5 nM) and R428 (1.3 µM, a concentration below its IC_{50}), PD-L1-si, R428 (a concentration below its IC_{50}), and cisplatin (5.35 µM, below its IC_{50}), cisplatin (5.35 µM), cisplatin (15.35 µM, a concentration below its IC_{50}), and untreated cells for 48 hours. Cell viability was assessed using the MTT assay which indicated that simultaneous blockade of *PD-L1* and *AXL* did not enhance the sensitivity of OVACAR-3 cells to cisplatin (*p=0.04, ***p=0.0003, ****p<0.0001, NS: Nonsignificant).

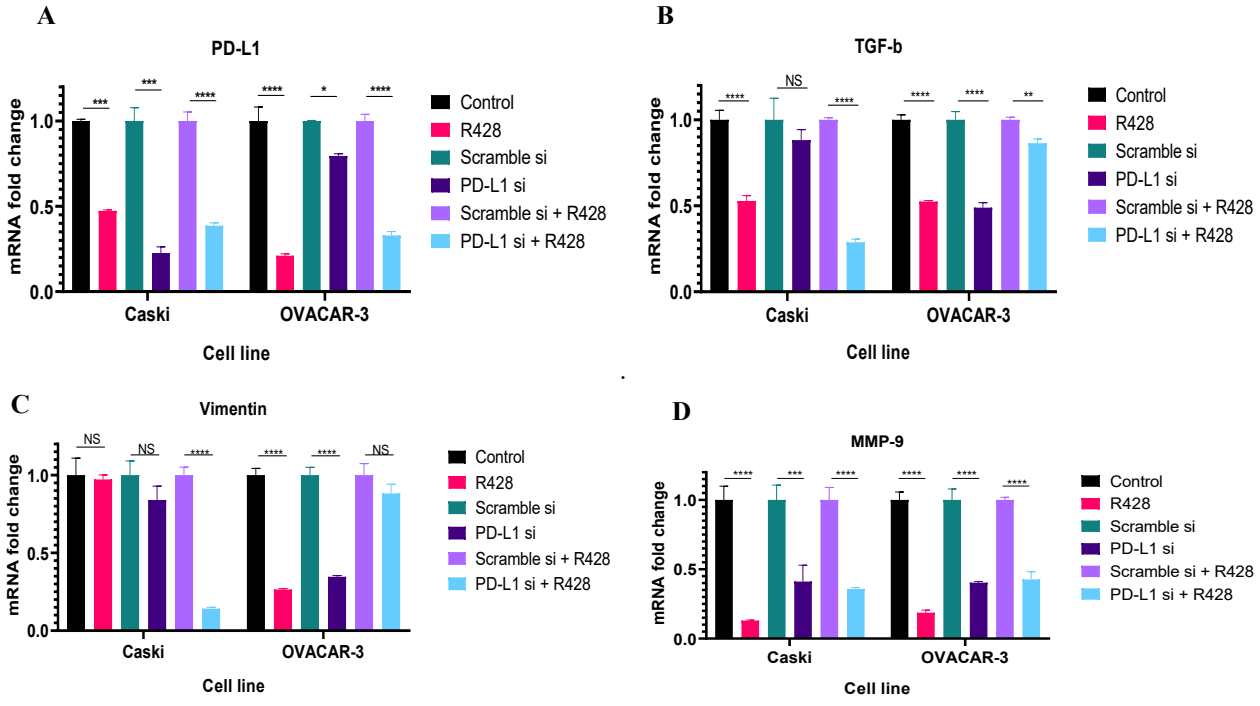

Figure 4. Expression of epithelial-mesenchymal transition (EMT)-related genes in OVACAR-3 and CaSki cells following treatment with PD-L1-siRNA and R428. A–D. Expression of *PD-L1*, *TGF-β*, *vimentin*, and *MMP-9* was reduced in OVACAR-3 and CaSki cells after treatment with PD-L1-siRNA and R428. Gene expression results are represented as mean ± SD of $2^{-\Delta\Delta Ct}$ after normalization with *HPRT* as an internal control (*p=0.01, **p=0.001, ***p=0.0005, ****p<0.0001, NS: Nonsignificant).

Simultaneous Blockade of PD-L1 and AXL Reduced CD44$^+$PD-L1$^+$ Cell Population

To evaluate the impact of blockade *PD-L1* and *AXL* on the invasive characteristics of the studied cell line, frequency of CD44$^+$PD-L1$^+$ cells was assessed using flow cytometry. Notably, the results showed a higher proportion of CD44$^+$PD-L1$^+$ cells in CaSki cells than in OVACAR-3 cells (Figure 5A). Co-treatment with *PD-L1* and R428 significantly diminished the frequency of CD44$^+$PD-L1$^+$ cells in CaSki cells but not in OVACAR-3 cells (Figure 5A–D).

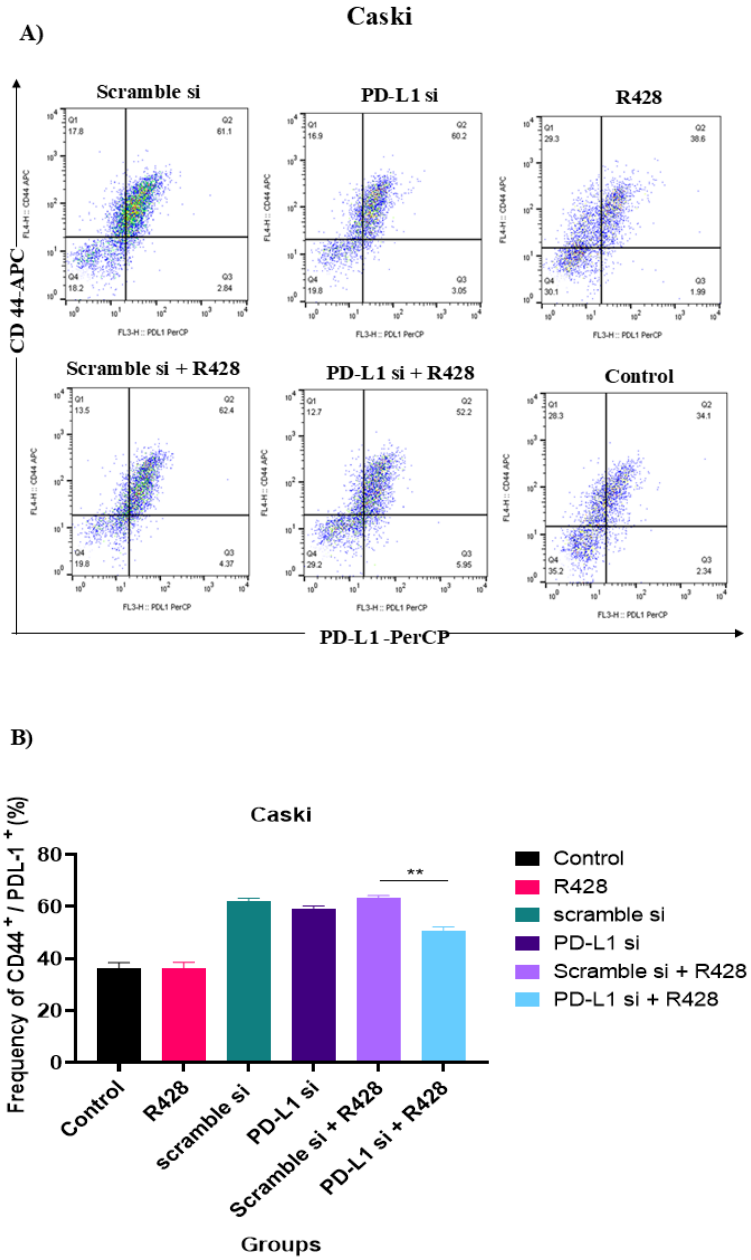

Published by Tehran University of Medical Sciences (http://ijaai.tums.ac.ir)

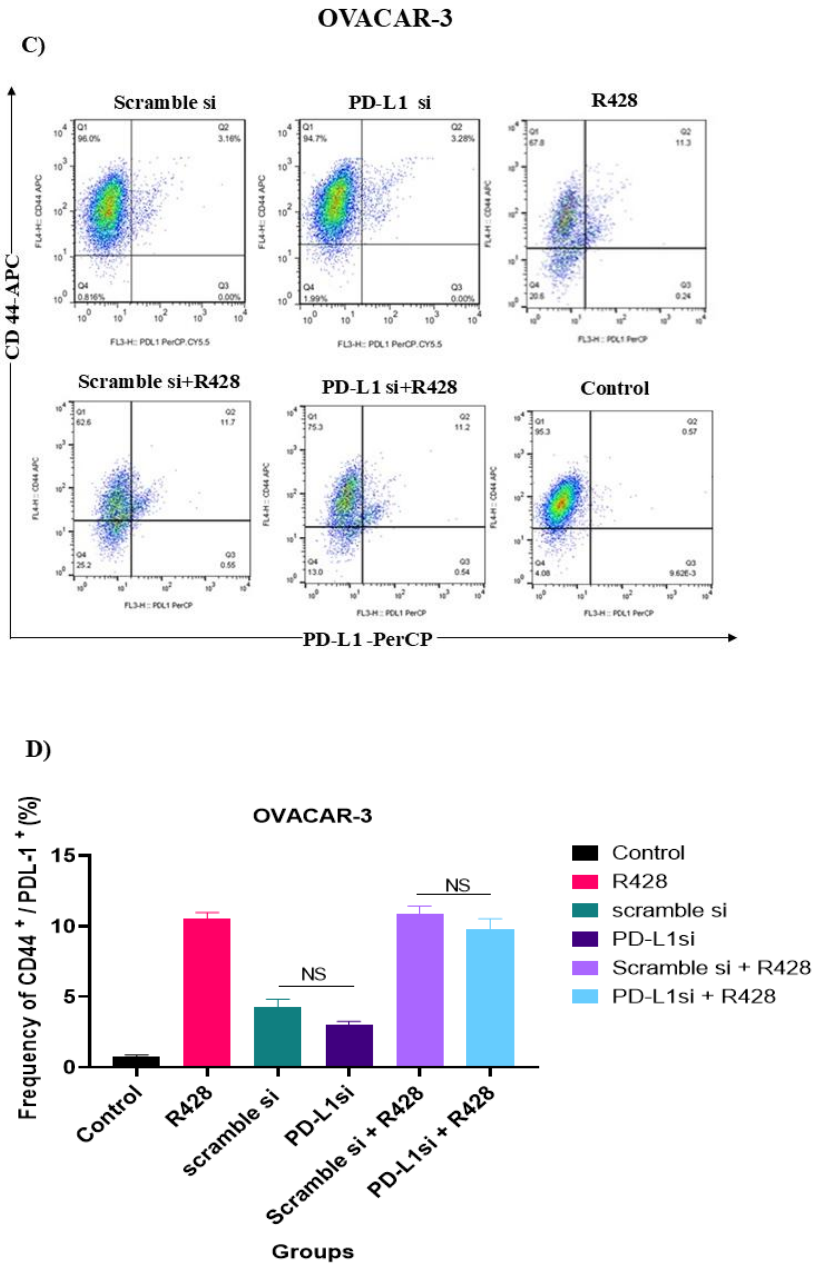

Figure 5. Percentages of CD44$^+$PD-L1$^+$ cells in OVACAR-3 and CaSki cells following treatment with PD-L1-siRNA and R428. Cells were stained with fluorochrome-conjugated monoclonal antibodies: Allophycocyanin (APC) anti-mouse/human CD44 and PerCP/Cyanine5.5 anti-human PD-L1 (BioLegend). Isotype-matched controls were used to define negative populations. Cells were incubated with antibodies for 30 minutes at 4 °C, washed twice with PBS, and analyzed using a FACS Calibur flow cytometer (BD Biosciences). Data were processed with FlowJo software. The combination treatment with PD-L1-siRNA and R428 significantly diminished the frequency of CD44$^+$PDL-1$^+$ cells in CaSki but not in OVACAR-3 cells. A. and C. Representative flow cytometric dot plots. B. and D. Quantification of CD44$^+$PD-L1$^+$ percentage in both cell lines (p=0.009, NS; Nonsignificant).**

Dual Blockade of PD-L1 and AXL Increased Apoptosis and Arrested Cell Cycle in Both OVACAR-3 and CaSki Cell Lines

Compared to the single treatment groups, flow cytometry using Annexin V-FITC/PI labeling showed remarkable apoptosis in both cell lines following combination treatment with PD-L1-siRNA and R428, particularly in OVACAR-3 cells, which exhibited more apoptosis. However, single treatment with PD-L1-si or R428 resulted in heightened cell apoptosis compared to the related control group (Figure 6A–D). Interestingly, the apoptotic cells were predominantly in the late and early phases of apoptosis in OVACAR-3 and CaSki cells, respectively (Figure 6A and 6C). Also, flow cytometry was performed to determine the effect of the treatments on the cell cycle of OVACAR-3 and CaSki cells. Co-treatment with PD-L1-si and R428 significantly induced G1 cell cycle arrest and prevented cells from entering the logarithmic phase of proliferation (S phase) in both cell lines in comparison with scramble-si+ R428 as a control group (Figure 7A–D). Additionally, cell cycle arrest was also determined in the sub-G1 area in the combined group, confirming apoptosis induction in CaSki cells (Figure 7A).

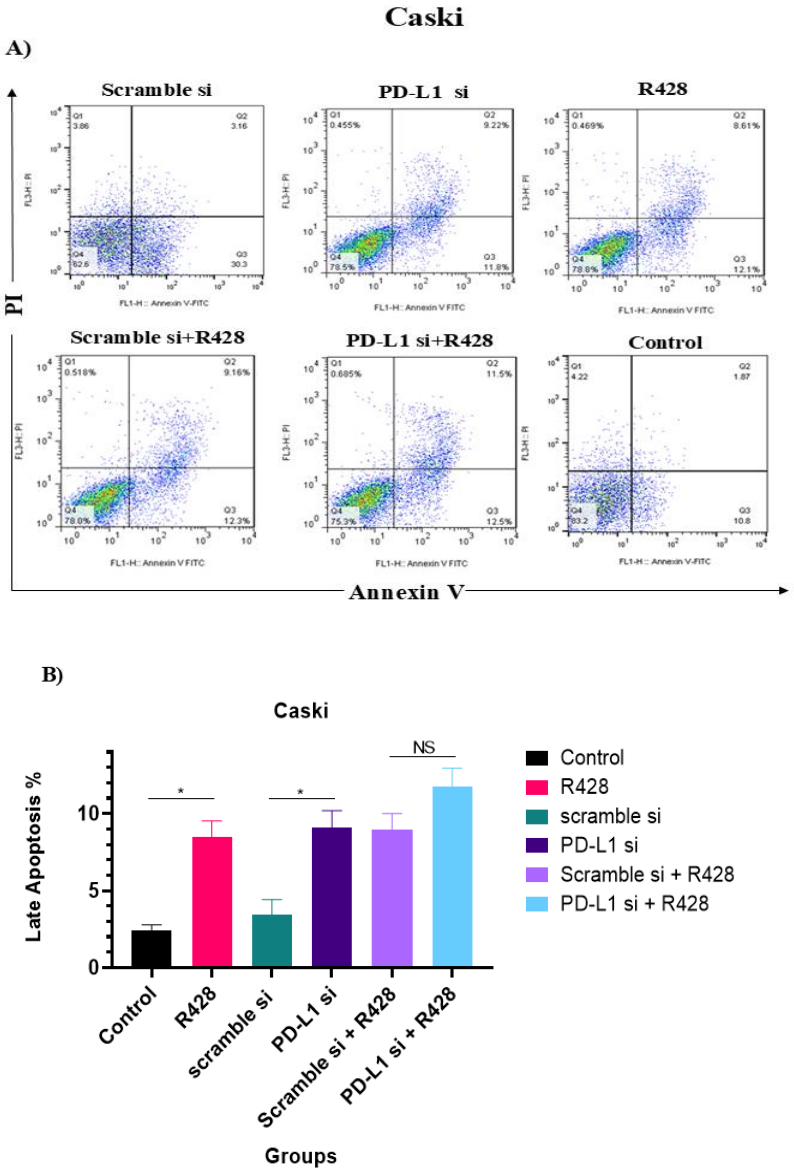

Published by Tehran University of Medical Sciences (http://ijaai.tums.ac.ir)

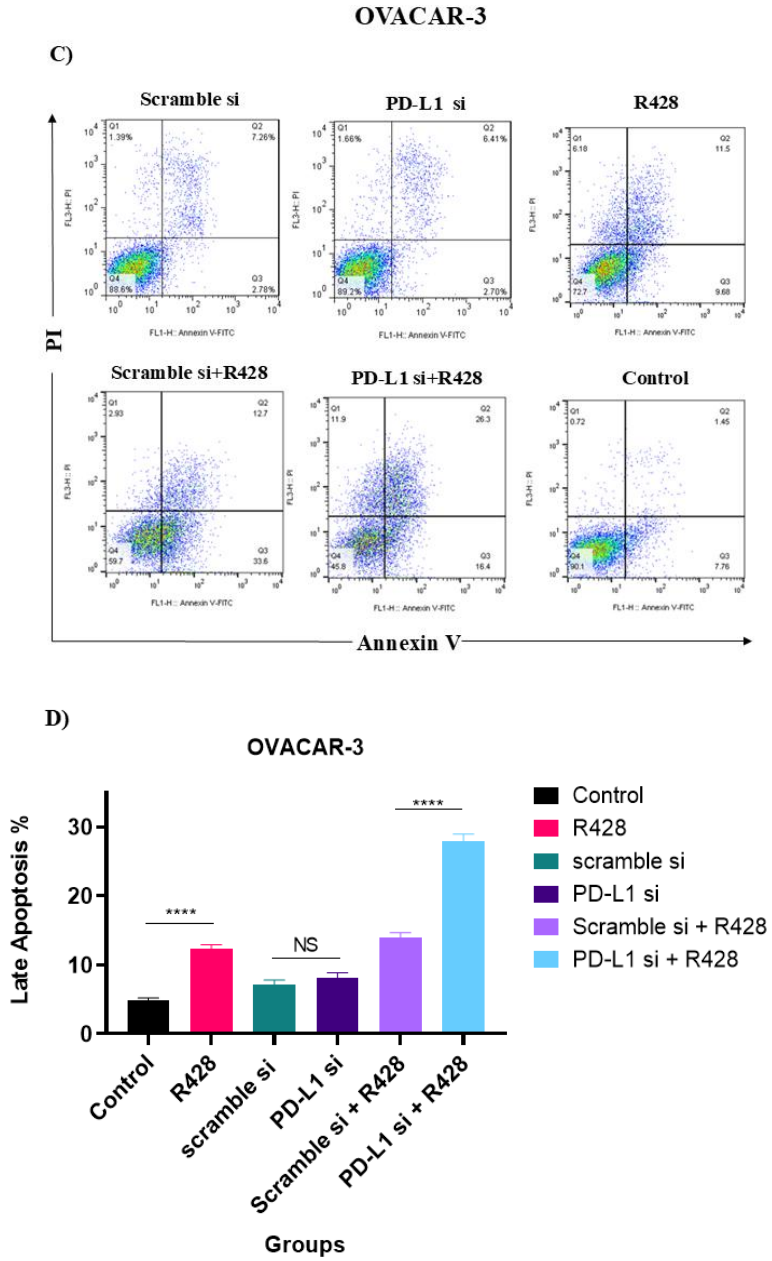

Figure 6. Both OVACAR-3 and CaSki cells showed increased apoptosis following treatment with PD-L1-siRNA and R428. Cells were treated for 48 hours, harvested, and stained with Annexin V-FITC (to detect phosphatidylserine externalization) and propidium iodide (PI) (to label dead cells) for 15 minutes in the dark. Samples were analyzed on a FACS Calibur flow cytometer. Quadrants distinguish viable (Annexin V−/PI−), early apoptotic (Annexin V+/PI−), late apoptotic (Annexin V+/PI+), and necrotic (Annexin V−/PI+) populations. A. and C. Annexin V-FITC/PI staining in OVACAR-3 and CaSki cells following treatment with PD-L1-siRNA and R428. B. and D. Quantification of apoptotic cells (late apoptosis). The combination treatment induced significant apoptosis in both cell lines compared to controls (p=0.01, ****p<0.0001).**

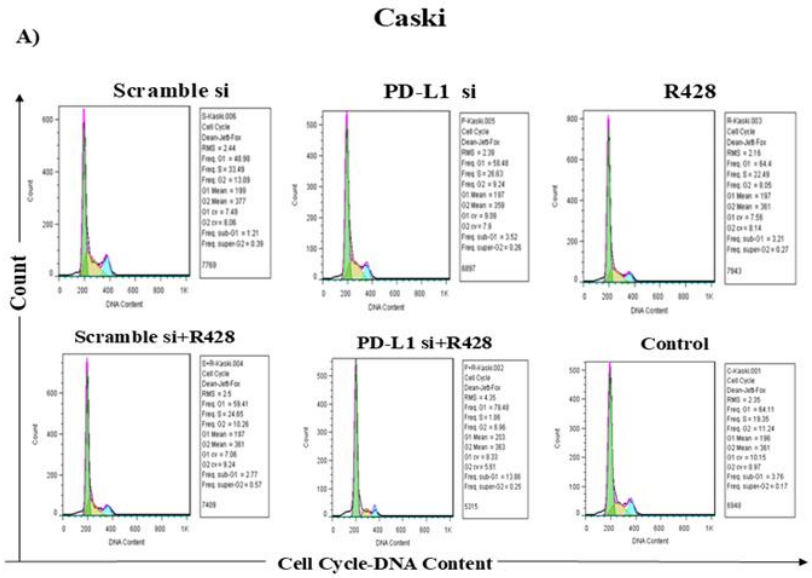
A)
Caski
Scramble si
PD-L1 si
R428
Scramble si+R428
PD-L1 si+R428
Control
Count
Cell Cycle-DNA Content

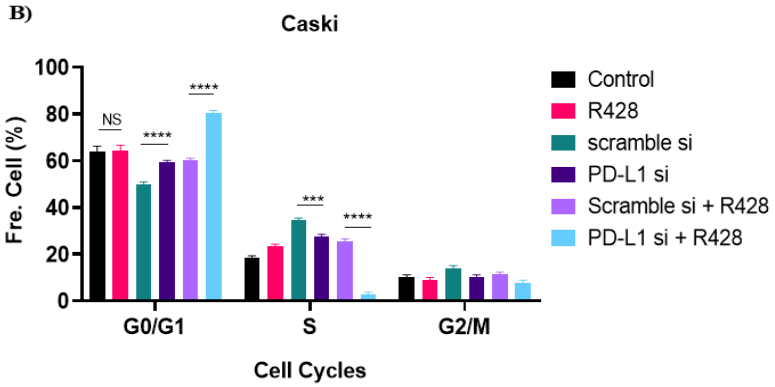
B)
Caski
Fre. Cell (%)
100
80
60
40
20
0
NS
****
****
***
****
G0/G1
S
G2/M
Cell Cycles
Control
R428
scramble si
PD-L1 si
Scramble si + R428
PD-L1 si + R428

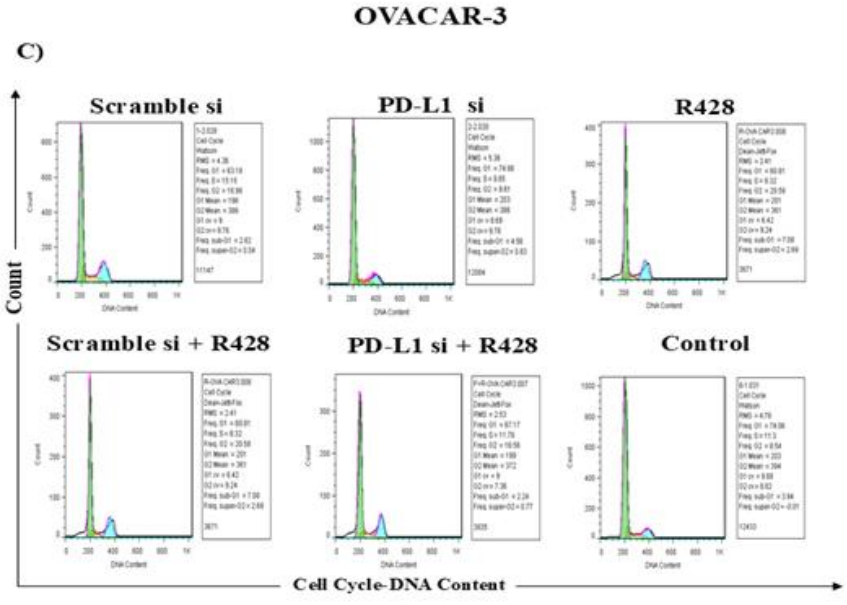
OVACAR-3
C)
Scramble si
PD-L1 si
R428
Scramble si + R428
PD-L1 si + R428
Control
Count
Cell Cycle-DNA Content

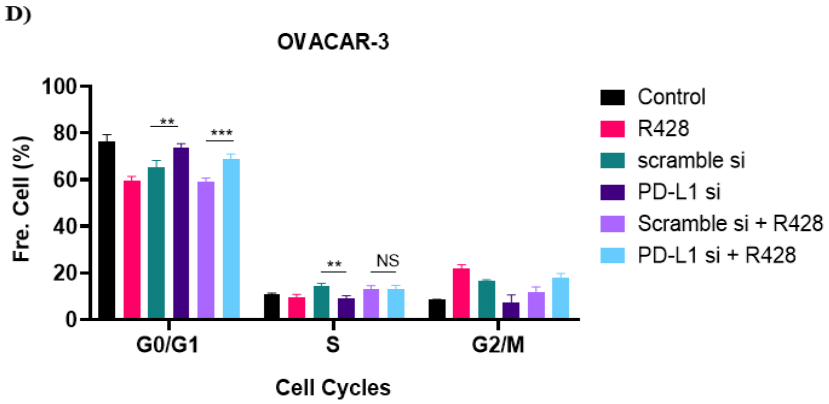

Figure 7. Effect of PD-L1-siRNA and R428 on cell cycle.

The cells were detached, washed with cold phosphate-buffered saline (PBS), stained with PI solution (50 µg/mL) and incubated in a dark place for 30 minutes. DNA content was analyzed using a FACS Calibur flow cytometer. Histograms depict cell cycle distribution (G0/G1, S, G2/M phases) and sub-G1 (apoptotic cells). A. and C. the combination treatment with PD-L1-siRNA and R428 induced G1 cell cycle arrest in OVACAR-3 and CaSki cells compared to cells treated with scramble siRNA and R428. B. and D. Graphs representing cell cycle status in both cell lines (p=0.002; ***p=0.0008; ****p<0.0001, NS; Nonsignificant).**

DISCUSSION

Despite the efficacy of conventional gynecologic cancer therapies, there is an urgent need for novel approaches, such as immunotherapy, to impede tumor invasion and counteract chemotherapy resistance.[1,3] ICBs targeting PD-L1 have emerged as a promising class of antitumor agents due to its pivotal role in immune evasion, cancer progression, EMT, and metastasis.[5] Nonetheless, ICBs cannot overcome all resistance mechanisms, limiting the proportion of cancer patients who benefit from ICB-based immunotherapy.[24,25] AXL, a receptor tyrosine kinase from the TAM family (including TYRO3, AXL, and MER), significantly promotes EMT-mediated cancer progression and chemoresistance through its dual functions in the tumor microenvironment and immune responses.[26,27]

Previous studies indicated a correlation between *AXL* expression and resistance to ICB therapy in tumor models and cancer patients.[10] Conversely, other studies on patients receiving tyrosine kinase inhibitors demonstrated the activation of the ERK pathway and increased expression of *PD-L1*, leading to the failure of those inhibitors and development of resistance.[9,28,29] Consequently, simultaneous blocking of *PD-L1* and tyrosine kinase is rational to augment the efficacy of targeted therapy.

Although PD-1/PD-L1 blockade therapy enhance clinical outcomes in cancer patients, their efficacy remains limited in many solid tumors, potentially due to off-target antibody binding as well as expression of PD-L1 on various cells, where it might play additional roles and be associated with poor prognosis.[5,16] Therefore, gaining a detailed understanding of the mechanisms influenced by *PD-L1* is crucial for developing an effective therapeutic strategy that directly targets cancer-related genes and modulates the signing pathways regulating cancer cell function.

AXL promotes tumor progression by dual mechanisms: (1) activating *PI3K/AKT/mTOR* and *ERK* signaling to drive EMT through *SNAIL/ZEB1* upregulation, and (2) creating an immunosuppressive microenvironment by inducing *PD-L1* expression.[10] Conversely, *PD-L1* exhibits both immune checkpoint function (mPD-L1) and tumor-intrinsic roles (cPD-L1), where cytoplasmic *PD-L1* activates *mTOR* to support cancer cell survival.[27,30] Some studies associate *PD-L1* with EMT, suggesting that overexpression of EMT-related genes, such as *AXL*, is linked to resistance to PD-1 therapy in melanoma.[31]

Also, Tsukita et al found that the AXL inhibitor, R428, reduced *PD-L1* and *CXCR6* expression in lung cancer cells, with minimal involvement of the *ERK* and *AKT* pathways.[10] Similarly, Yu et al revealed that PD-L1-siRNA modulates lung cancer cell proliferation

through the *PI3K/AKT/mTOR* and *ERK* signaling pathways.[30]

In the current study, we initially verified that expression levels of *PD-L1*, *AXL*, and certain EMT-regulating genes were elevated in OVACAR-3 and CaSki cells compared to other examined cell lines. This suggests that OVACAR-3 and CaSki cells may exhibit higher sensitivity to the blockade of *PD-L1* and EMT-related genes. Additionally, we observed a significant decrease in the proliferative ability of OVACAR-3 and CaSki cells following *PD-L1* and *AXL* blockade with both PD-L1-siRNA alone and in combination with R428 effectively inhibited cancer cell proliferation, indicating that *PD-L1* upregulation may play a crucial role in cancer cell growth. Similarly, it has been shown that combining the selective AXL kinase inhibitor, BGB324, with anti-PD-1 effectively reduced tumor progression in mice bearing KPL tumors, a genetically engineered model with mutant *Kras/Tp53*.[14] Likewise, Li et al showed that combining PD-L1-siRNA with imatinib inhibited the proliferation of B16F10 melanoma cells. Moreover, in the mice bearing B16 melanomas, this combination therapy markedly reduced the size and growth rate of the tumor.[32] Tian et al showed that combined treatment of cisplatin and R428 significantly enhanced the inhibitory effect of cisplatin on HO-8910 and SKOV3.ip ovarian cancer cells.[33] Also, Oien et al demonstrated that silencing *AXL* or blocking its activation with BGB324 enhanced sensitivity of malignant pleural mesothelial (MPM) cells to cisplatin and pemetrexed.[34] Inconsistently, we found that the combination of R428 along with PD-L1-siRNA was insufficient to overcome cisplatin resistance in the OVACAR-3 cell line, while it reduced expression of *TGF-β*, *vimentin*, and *MMPs*, key EMT-regulating genes involved in tumor cell migration and metastasis. Similarly, Yu et al reported that knockdown of *PD-L1* reduced the expression of *N-cadherin*, *vimentin*, *MMP-9*, and *claudin-1* while increasing *E-cadherin* expression in lung cancer cells.[30] Also, blockade of the *PD-L1* and *JAK/STAT3* signaling pathways has been suggested to reduce migration and EMT in prostate cancer cells,[35] and R428 treatment was shown to downregulate both *MMP2* and *MMP9* in TE1 esophageal carcinoma cells.[36]

PD-L1 plays an essential role in prompting stem cell-like characteristics in cancer cells.[37] Additionally, *CD44*, a well-known cancer stem cell marker, has been associated with tumor development and invasion.[38] An analysis of 119 archival ovarian cancer samples revealed a correlation between *PD-L1* expression and elevated levels of stem cells markers, including *CD44* and *LGR5*.[39] Moreover, Zhang et al demonstrated that $CD44^{+}CD24^{+}$ cervical cancer cells may exhibit resistance to radiation therapy and a greater incidence of recurrence and distant metastasis.[40] Therefore, we investigated the frequency of $CD44^{+}PD\text{-}L1^{+}$ cell populations in cancer cells subjected to combination treatment. Our data revealed a substantial decrease in the population of invasive $CD44^{+}PD\text{-}L1^{+}$ cells in treated CaSki cells; however, this reduction was not statistically significant in OVACAR-3 cells.

We also observed an increased apoptotic activity in cells subjected to simultaneous blockade of *PD-L1* and *AXL*. Similarly, Teo et al showed SKOV3 cells treated with PD-L1 siRNA exhibited increased sensitivity to apoptosis compared to the control cells.[19] Also, Li et al suggested that combined delivery of PD-L1-siRNA and Imatinib (as a TKI) on B16F10 melanoma cells could reduce tumor cell proliferation and induce apoptosis.[32] Consistently, the AXL inhibitor R428 was shown to increased TRAIL-mediated apoptosis through downregulation of *c-FLIP* and *survivin* expression in renal carcinoma cells.[41]

In our study, proliferation of OVACAR-3 and CaSki cells was arrested at the G0/G1 phase of the cell cycle, following simultaneous blockade of *PD-L1* and *AXL*. Consistent with this, Li et al suggested that knockdown of *PD-L1* in SGC-7901 and AGS cell lines could induce the cell cycle arrest in the G0/G1 phase.[42] Similarly, it was reported that a dual MET/AXL small-molecule inhibitor caused cell cycle arrest at the G1 phase by reducing the expression of cell cycle regulatory factors like *Cyclin A2* and *Cyclin D1*.[7]

In our study, CaSki cells exhibited greater sensitivity to growth inhibition by simultaneous blockade of *PD-L1* and *AXL* suggesting an elevated cytoplasm *PD-L1* (cPDL1) expression relative to OVACAR-3 cells. Concurrently, transcriptomic analysis of ovarian cancer samples has demonstrated that *AXL* expression levels correlate with the sensitivity of ovarian cancer patients to cisplatin chemotherapy.[33] Cell viability assay in our study showed that OVACAR-3, as a chemoresistant cancer cell line, sustained cisplatin resistance, while we proposed synergistic effect of PD-L1-siRNA combined with AXL inhibitor to mitigate drug resistance.

We also demonstrated that OVACAR-3 cells have a diminished reduction of genes associated with EMT, probably due to the proven high aggressive

characteristics and underlying chemoresistance.[43] CaSki cells exhibited a dramatic correlation between *CD44* and *PD-L1* expression, in contrast to the OVACAR-3 cell line, highlighting differences in *PD-L1* distribution and the predominance of membrane *PD-L1* (mPD-L1) in CaSki cells. Finally, we observed a minor arrest in the G0/G1 in OVACAR-3 cells, confirming cell viability assay data that exhibit more resistance to growth inhibition following combined therapy.

In this study, we used CaSki and OVACAR-3 cells, the two gynecologic cancer cell lines with distinct impact values and behaviors. As a result, the primary innovation of our study lies in demonstrating the therapeutic potential of this combination therapy across two cancers.

Numerous studies suggest that *PD-L1* is distributed across various cellular components, including mPD-L1, cPD-L1, nuclear *PD-L1* (nPD-L1), and serum *PD-L1*.[44-49] Our results demonstrated that CaSki cells exhibit high levels of both mPD-L1 and cPD-L1, whereas OVACAR-3 cells express cPD-L1 but lack mPD-L1, as previously reported.[50] The form of *PD-L1* has been shown to affect antitumor immune responses.[16,51] Consequently, as a second novel finding, we found gene silencing using siRNA is particularly relevant due to positive cPD-L1 expression in both cell lines. However, given the predominant expression of mPD-L1 in CaSki cells, using anti-PD-L1 antibodies may also be beneficial to counteract tumor invasiveness.

This study highlights the potential of co-targeting *PD-L1* and *AXL* in gynecological cancers; however, its findings are limited to in vitro models, and in vivo validation is necessary. The mechanistic roles of *PD-L1* isoforms and mechanisms underlying cisplatin resistance in OVACAR-3 cells were not fully explored. Future research should investigate combination therapies with pathway inhibitors, such as *PI3K/AKT* or *JAK/STAT*, and utilize gene-editing tools, such as CRISPR, to enhance therapeutic outcomes.

In this study, we successfully reduced key characteristics of tumor progression through simultaneous blockade of *PD-L1* and *AXL* in OVACAR-3, an ovarian cancer cell line, and CaSki, a cervical cancer cell line. Our findings demonstrated that *AXL*-targeted treatment in *PD-L1*-expressing cell lines has significant potential to overcome resistance to ICBs and might expand the range of patients who could benefit from combination-targeted therapies. Further studies will be needed to thoroughly explore immunological mechanism in different contexts when proposing *PD-L1* and RTK blockers as a novel approach to cancer immunotherapy.

STATEMENT OF ETHICS

This study was found to be ethically acceptable by the Ethical Committee of Mazandaran University of Medical Sciences (IR.MAZUMS.REC.1400.620)

FUNDING

This study was supported in part by grants provided by Mazandaran University of Medical Sciences and Shahid Sadoughi University of Medical Sciences. Project number 11648.

CONFLICT OF INTEREST

The authors declare no conflicts of interest.

ACKNOWLEDGMENTS

We sincerely appreciate Dr. Misagh Rajabinejad for their excellent advice and valuable insights, which greatly contributed to the development of this work.

DATA AVAILABILITY

Upon reasonable request (specify contact method).

AI ASSISTANCE DISCLOSURE

Language refinement and paraphrasing support for this manuscript were partially provided using QuillBot software.

REFERENCES

1. Cohen PA, Jhingran A, Oaknin A, Denny L. Cervical cancer. Lancet. 2019;393(10167):169–82.
2. Stewart C, Ralyea C, Lockwood S. Ovarian cancer: An integrated review. Semin Oncol Nurs. 2019;35(2):151–6.
3. Jiang G, Wu Q, Li B. Evaluation of immunotherapy efficacy in gynecologic cancer. Front Immunol. 2023;14:1061761.
4. Wherry EJ, Kurachi M. Molecular and cellular insights into T cell exhaustion. Nat Rev Immunol. 2015;15(8): 486–99.

5. Akinleye A, Rasool Z. Immune checkpoint inhibitors of PD-L1 as cancer therapeutics. J Hematol Oncol. 2019;12(1):92.
6. Yang Y, Wang L, Han R, Wang Q, Zhang G, Liu H, et al. Protein tyrosine kinase inhibitor resistance in malignant tumors: Molecular mechanisms and future perspective. Signal Transduct Target Ther. 2022;7(1):329.
7. Zhu C, Wei Y, Wei X, Wang D, Zheng Z, Zhang Y, et al. A dual MET/AXL small-molecule inhibitor exerts efficacy against gastric carcinoma. MedComm (2020). 2020;1(1):103–18.
8. Bakir B, Chiarella AM, Pitarresi JR, Rustgi AK. EMT, MET, plasticity, and tumor metastasis. Trends Cell Biol. 2020;30(10):764–76.
9. Skinner HD, Sandulache VC, Ow TJ, Meyn RE, Yordy JS, Beadle BM, et al. AXL-PI3K-PD-L1 signaling axis and radiation resistance. Clin Cancer Res. 2017;23(11):2713–22.
10. Tsukita Y, Fujino N, Miyake K, Tsurudome Y, Araki T, Ohsaki Y, et al. Axl kinase drives immune checkpoint and chemokine signalling in lung adenocarcinomas. Mol Cancer. 2019;18(1):24.
11. Jin H, Wang L, Bernards R. Rational combinations of targeted cancer therapies. Nat Rev Drug Discov. 2023;22(3):213–34.
12. Yang C, Xia BR, Zhang ZC, Zhang YJ, Lou G. Immunotherapy for ovarian cancer: Adjuvant, combination, and neoadjuvant. Front Immunol. 2020;11:577869.
13. Iinuma K, Saito K, Hirano Y, Suzuki Y, Nagai K, Tanaka H, et al. Combination therapy in metastatic renal cell carcinoma. Cancers (Basel). 2023;15(3):–.
14. Li H, Li Y, Liu H, Shi Y, Zhang Y, Liang Q, et al. AXL targeting restores PD-1 blockade sensitivity in NSCLC. Cell Rep Med. 2022;3(3):100554.
15. Li J, Wang J, Chen X, Zhao Y, Zhang L, Xu Y, et al. ICIs and TKIs in advanced colorectal cancer: Meta-analysis. Oncol Lett. 2024;27(4):153.
16. Wu Y, Chen W, Xu Z, Zhao Z, Wang X. PD-L1 distribution and perspectives for cancer immunotherapy. Front Immunol. 2019;10:2022.
17. Hu B, Weng Y, Xia XH, Liang XJ, Huang Y. Therapeutic siRNA: State of the art. Signal Transduct Target Ther. 2020;5(1):101.
18. Ozcan G, Ozpolat B, Coleman RL, Sood AK, Lopez-Berestein G. Development of siRNA-based therapeutics. Adv Drug Deliv Rev. 2015;87:108–19.
19. Teo PY, Yang C, Guo X, Liu X, Shen J. PD-L1 siRNA delivery for ovarian cancer immunotherapy. Adv Healthc Mater. 2015;4(8):1180–9.
20. Kang SW, Choi HJ, Cho M, Shin H, Kim YK. Transcriptome profiling of ovarian cancer xenografts. Sci Rep. 2024;14(1):11894.
21. Lee EH, Kim JY, Jeong JH, Choi JW, Kim YJ. Axl blockade in HPV16E6-mediated cervical cancer. Sci Rep. 2017;7(1):5759.
22. Mujoo K, Kipps TJ, Yang HM, Cherney B, Larrick JW. Emergence of cisplatin-resistant OVCAR-3 cells. Int J Gynecol Cancer. 2000;10(2):105–14.
23. Wang L, Xu W, Zhang L, Hu J, Xia X. Drug resistance in ovarian cancer: Mechanisms to clinical trials. Mol Cancer. 2024;23(1):66.
24. Nagasaki J, Ishino T, Togashi Y. Mechanisms of resistance to immune checkpoint inhibitors. Cancer Sci. 2022;113(10):3303–12.
25. Santoro A, Angi M, Camarda F, Dellino M, Bogani G. Role of PD-L1 in gynecological cancers. Gynecol Oncol. 2024;184:57–66.
26. Bhalla S, Gerber DE. AXL inhibitors: Status of clinical development. Curr Oncol Rep. 2023;25(5):521–9.
27. Liu Y, Li X, Zhang Y, Qian J, Yang L. AXL and the immunosuppressive microenvironment. Mol Cancer. 2025;24(1):11.
28. Yang M, Li X, Yu X, Hu W, Zhang J. Cancer immunotherapy resistance: Mechanisms and biomarkers. Cell Commun Signal. 2024;22(1):338.
29. Tanaka T, Fujiwara T, Saito Y, Kudo M, Nakamura M. Anti-PD-L1 promotes proliferation via PD-L1–AXL in liver cancer. Hepatol Int. 2024;18(3):984–97.
30. Yu W, Zhang X, Chen G, Xu R, Wang S. PD-L1 activates WIP and β-catenin in lung cancer. Cell Death Dis. 2020;11(7):506.
31. Boshuizen J, Vredevoogd DW, Krijgsman O, Ligtenberg MA, de Bruijn B, Jimenez CR, et al. AXL-ADC and ICB in melanoma and lung cancer. Cancer Res. 2021;81(7):1775–87.
32. Li C, Han X. Melanoma immunotherapy with PD-L1 siRNA and imatinib. Pharm Res. 2020;37(6):109.
33. Tian M, Wang H, Wang J, Zhang W, Chen Q. AXL inhibition sensitizes ovarian cancer to cisplatin. Acta Pharmacol Sin. 2021;42(7):1180–9.
34. Oien DB, Pathoulas CL, Ray U, Shi R, Conejo-Garcia JR, Lengyel E, et al. AXL inhibitor enhances mesothelioma cell death. Front Pharmacol. 2017;8:970.
35. Bastaki S, Bae DH, Mecham B, Richardson DR, Huang

ML. Codelivery of STAT3 and PD-L1 siRNA suppresses cancer. Life Sci. 2021;266:118847.
36. Han S, Wang H, Zhang C, Liu L, Li S. AXL inhibition suppresses esophageal carcinoma growth. Exp Ther Med. 2020;20(5):41.
37. Almozyan S, Colak D, Mansour F, Alaiya A, Ghebeh H. PD-L1 promotes stemness in breast cancer. Int J Cancer. 2017;141(7):1402–12.
38. Idowu MO, Kmieciak M, Dumur CI, Burton RS, Grimes MM, Powers CN, et al. CD44+/CD24−/low cells in triple-negative breast cancer. Hum Pathol. 2012;43(3):364–73.
39. Alwosaibai K, Zakaria Z, Yahaya BH, Abdullah H, Lim KP. PD-L1 and cancer stem cells in ovarian cancer. BMC Cancer. 2023;23(1):13.
40. Zhang J, Ding L, Tian Y, Li X, Yu S. CSC-like traits in cervical cancer and radioresistance. Gynecol Obstet Invest. 2019;84(2):174–82.
41. Woo SM, Min KJ, Kim S, Park JW, Kim DE, Kim SH, et al. AXL inhibitor R428 enhances TRAIL-induced apoptosis. Int J Mol Sci. 2019;20(13):–.
42. Li J, Xu J, Yan X, Jin K, Li W. PD-L1 knockdown in gastric cancer cells. Cell Physiol Biochem. 2017;41(3):907–20.
43. Mitra AK, Davis DA, Tomar S, Roy A, Gurler H, Xie JL, et al. In vivo growth of ovarian cancer cell lines. Gynecol Oncol. 2015;138(2):372–7.
44. Chowdhury S, Matin K, Ali M, Paul P, Rahman M. PD-L1 as a marker in thyroid cancer. Oncotarget. 2016;7(22):32318–28.
45. Ghebeh H, Tulbah A, Mohammed S, Elkum N, Bin Amer S, Alaiya A, et al. Doxorubicin modulates PD-L1 expression. Breast Cancer Res. 2010;12(4)\:R48.
46. Hua D, Zheng S, Xu G, Yuan X, Zhang B, Chen Y, et al. B7-H1 and regulatory T cells in colorectal cancer. World J Gastroenterol. 2012;18(9):971–8.
47. Satelli A, Batth IS, Brownlee Z, Mitra A, Zhou S, Rojas C, et al. Nuclear PD-L1 in circulating tumor cells. Sci Rep. 2016;6:28910.
48. Tang Y, Fang W, Zhang Y, Hong S, Kang S, Yan Y, et al. PD-L1, EGFR and prognosis in NSCLC. Oncotarget. 2015;6(16):14209–19.
49. Ukpo OC, Thorstad WL, Lewis JS Jr. B7-H1 in HPV-related oropharyngeal cancer. Head Neck Pathol. 2013;7(2):113–21.
50. Qu QX, Xie F, Huang Q, Zhang XH, Xie J, Wang XH, et al. PD-L1 expression in ovarian cancer. Cell Physiol Biochem. 2017;43(5):1893–906.
51. Parvez A, Alam M, Hamid AS, Suhail M, Ahmad A. PD-1 and PD-L1 in cancer immunotherapy. Front Immunol. 2023;14:1296341.